Available online at www.sciencedirect.com
SCIENCE DIRECT
Nuclear Instruments and Methods in Physics Research A 564 (2006) 752–760
NUCLEAR INSTRUMENTS & METHODS IN PHYSICS RESEARCH Section A
www.elsevier.com/locate/nima

Combined application of multielement analysis—k_0-INAA and PIXE—and classical techniques for source apportionment in aerosol studies

S.M. Almeida[a,*], M.C. Freitas[a], M.A. Reis[a], C.A. Pio[b], M.A. Trancoso[c]

[a]*ITN-Reactor, Technological and Nuclear Institute, E.N. 10, 2686-953 Sacavém, Portugal*
[b]*DAO-Aveiro University, Campus Universitário de Santiago, 3810-193 Aveiro, Portugal*
[c]*LAACQ-Instituto Nacional de Engenharia, Tecnologia e Inovação,Estrada do Paço do Lumiar 22, 1649-038 Lisboa, Portugal*

Available online 2 May 2006

Abstract

Three objectives were proposed in this work: (i) to evaluate the concentrations of Air Particulate Matter (APM) species obtained via k_0-INAA and PIXE by comparison with results obtained via classical methodologies, (ii) to study the water solubility of chloride, sodium, sulfur, potassium and calcium sampled in APM filters and (iii) to analyze the importance of their solubility in the identification of emission sources. The multi-technique analytical approach, using nuclear and classical techniques, not only the results provided for a large number of APM species (essential for source apportionment studies) but also, for several elements, independent methods gave information about their solubility. Results indicated that: (1) the total Cl concentration was lower than the soluble Cl^- concentration, showing that it volatilized partially during the PIXE analysis, (2) the majority of Na—provided mainly from sea salt spray—was soluble, (3) in PM_{10} most of the sulfur was in SO_4^{2-} chemical form, (4) K exhibited aweaker solubility in the coarse fraction: in $PM_{10-2.5}$, the insoluble potassium was associated with the mineral aerosol, whereas the soluble fraction resulted from the sea salt spray, (5) Ca showed a lower solubility in the coarse fraction, and the insoluble Ca was associated with a mineral origin.

PACS: 29.30.Kv; 07.88.+y

Keywords: Air particulate matter; $Pm_{2.5}$; Pm_{10}; Solubility; Principal component analysis

1. Introduction

Airborne trace elements are important because of their association with environmental issues and health of plants, animals and humans. Several reports reveal significant correlations between Air Particulate Matter (APM) levels and increased respiratory and cardiovascular diseases, and mortality [1–4]. Consequently, APM studies are extremely important in areas affected by pollution sources, mainly when they are very populated. Considerations must be given to the elements' essentiality, non-essentiality and toxicity, which depend on their concentrations and chemical forms (speciation) and on pH and oxidation–reduction conditions [5].

In industrial areas, due to the lack of adequate emission inventories, measurements of aerosol constituents seem to be a practical way to provide information about pollution sources using multivariate receptor modeling techniques, especially as the quantity and the quality of speciated APM data increase. Multivariate receptor modeling approaches are based on the idea that time dependence of a chemical species at the receptor site will be the same for the chemical species from the same source. Chemical species are measured in a large number of samples gathered at a single receptor site over time. Species of similar variability are grouped together in a minimum number of factors that explain the variability of the data set. It is assumed that each factor is associated to a source type.

*Corresponding author. Tel.: +351 21 9946130; fax: +351 21 9946153.
E-mail address: smarta@itn.pt (S.M. Almeida).

0168-9002/$ - see front matter © 2006 Elsevier B.V. All rights reserved.
doi:10.1016/j.nima.2006.04.007

Numerous studies have been carried out whereby the sources and chemical composition of rural, urban and industrialized APM have been investigated [6–11]. However, only a few studies analyzed the importance of the elements solubility in the identification of sources.

2. Experimental

2.1. Site description

APM was sampled in a sub-urban area located in the outskirts of Lisbon (latitude 38°48′ 50″N, longitude 9° 05′ 29″W). This site is situated 10 km northeast from the urban centre of Lisbon and 20 km northeast from the Atlantic Ocean. The sampling site is surrounded by a heavy traffic road (about 10 m east), by the Tagus Estuary (1 km east), by the International Airport (about 5 km southwest) and to the north by an industrial region (urban waste incinerator, fuel-powered station and chemical, food, glass, and cement industries) (Fig. 1).

2.2. Description of the sampling equipment

APM was collected with two samplers operating side by side—one low volume sampler and one high volume sampler—during 24 h periods and on a twice a week basis.

The low-volume—Gent PM_{10} sampler—was equipped with a Stacked Filter Unit (SFU) which carried two 47 mm Nuclepore polycarbonate filters, with 8 and 0.4 μm pore size, in two different stages. Upstream of the coarse filter was a pre-impactor stage. At a flow rate of 15–16 L min^{-1}, a pre-impaction stage intercepted particles larger than about 10 μm aerodynamic diameter (AD), and the filter with 8 μm pore size (coarse filter) had a 50% collection efficiency at about 2.5 μm AD. A detailed description of the sampling equipment is given by Maenhaut [12].

The high volume sampler was equipped with a Sierra PM_{10} size selective inlet and a Sierra single stage impactor plate to separate particles in two size fractions: $2.5 < AD < 10$ μm and $AD < 2.5$ μm. This sampler operated at a flow rate of 1.13 m^3 min^{-1}. Aerosol samples were collected on pre-treated and washed Whatman QM-A quartz fiber filters [13].

2.3. Gravimetric and chemical analysis

Nuclepore filters were weighed before and after sampling on a 0.1 μg sensitivity balance. For elemental analysis, filters were cut into three parts: half was analyzed by k_0-INAA [14,15], a quarter was analyzed by PIXE [16] and the last quarter was kept for other possible measurements or replicates. For k_0-INAA analysis, filter halves were rolled up and put into a thin foil of aluminium and irradiated for 7 h at a thermal neutron flux of 1.2×10^{13} cm^{-2} s^{-1} in the Portuguese Research Reactor. After irradiation the sample was removed from the aluminium foil and transferred to a polyethylene container. For each irradiated sample, two gamma spectra were measured with hyperpure germanium detectors, one spectrum 2–3 days after irradiation and the other one after 4 weeks. The k_0 method was used and 1 mm diameter wires of 0.1% Au–Al were co-irradiated as comparators. PIXE analysis was carried out at a Van de

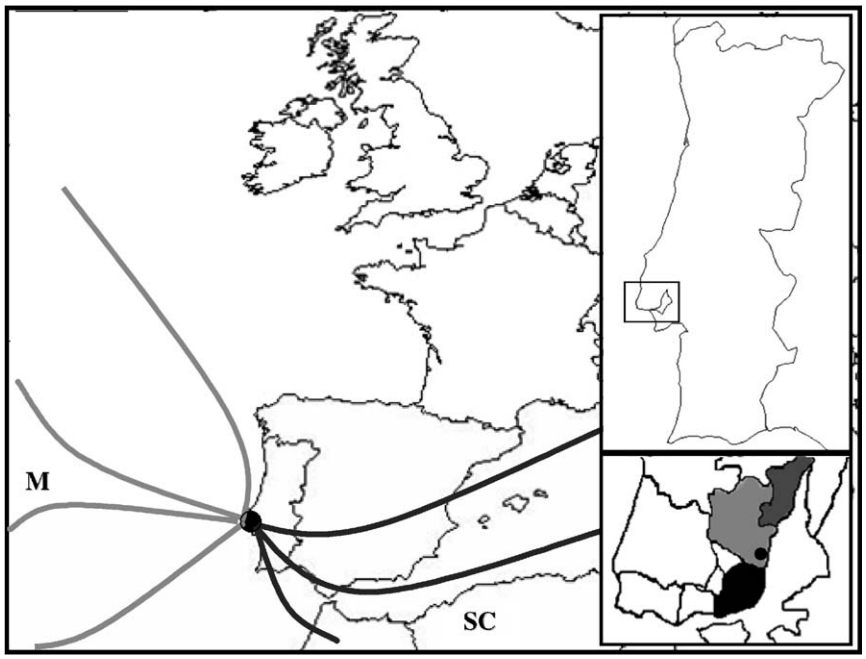

Fig. 1. Sampling site localization ● (Black pattern—urban centre of Lisbon. Light and dark grey patterns—Loures and Vila Franca de Xira suburban/industrial areas on the right margin of the Tagus Estuary, concentrating the Lisbon industrial congregate). Air mass categorization, based on four day backward trajectories obtained from Hysplit model. M—Maritime; SC—South Continental.

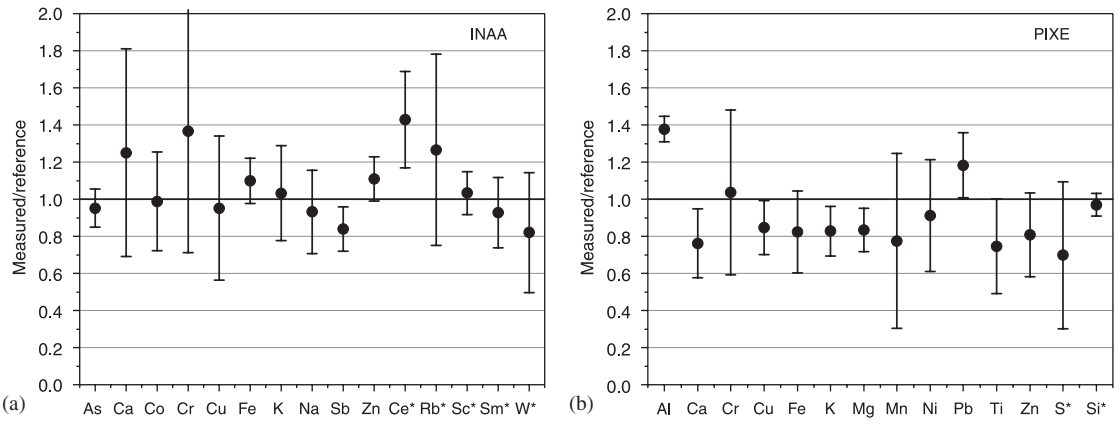

Fig. 2. Determined/certified or determined/indicative (*) ratios in NIST CRM 2783 filters measured by k_0-INAA (a) and PIXE (b). Uncertainties are at 95% confidence level for 3 replicates. One single replicate for Ca determined by k_0-INAA and the uncertainty refers to the counting statistical error.

Graaff accelerator, in vacuum and two X-ray spectra were taken for each of the samples: one with a 1.2 MeV proton beam and no absorber in front of the Si(Li) detector for low energy X-ray elements and another with a 2.4 MeV proton beam and a 250 μm Mylar® filter to detect elements with atomic number higher than 20. Previously to the sampling campaign, tests of reproducibility within filters and between filters were taken, using parallel sampling with two similar sampling units and measuring the particle species by k_0-INAA and PIXE. Results were reproducible to within 5–15%, providing strong support for the validity of the analytical techniques. The accuracy of analytical methods was evaluated with NIST filter standards (Fig. 2). For k_0-INAA, except for Ca and Cr, results reveal an agreement of $\pm 10\%$ for the certified elements. For PIXE, except for Al and Pb, the resulting values have a good precision but fall systematically 20% under the certified value. The details of sampling and analytical control tests and detection limits were given in previous works [17–20].

The complementary of k_0-INAA and PIXE techniques allowed the determination of elemental concentrations for 37 elements. Na, Sc, Fe, Co, Zn, As, Sb, La and Sm determined by k_0-INAA and Al, Si, S, Cl, K, Ca, Ti, V, Mn, Ni, Cu, Br and Pb determined by PIXE could be measured in more than 80% of the samples, both fine and coarse fractions, and they were retained for further data processing.

Quartz fiber filters were weighed before and after sampling on a 10 μg sensitivity balance. One portion of the filter was extracted with distilled deionized water by ultrasonic and mechanical shaking and filtered through a pre-washed Whatman 42 filter. The aqueous extract was analyzed by Ion Chromatography [21] (Cl^-, NO_3^- and SO_4^{2-}), Indophenol-blue Spectrophotometry [22] (NH_4^+), Atomic Absorption Spectroscopy [23] (Ca^+, Mg^{2+}, Na^+ and K^+), and Potentiometry (H^+). Black carbon (BC) and organic carbon (OC) contents were determined in another portion of the quartz fiber filters with a thermo-optical system, based on the thermal desorption/oxidation to CO_2 with subsequent determination by non-dispersive infrared spectrophotometry [24].

Blank Nuclepore and quartz filters were treated the same way as regular samples. All measured species were very homogeneously distributed; therefore concentrations were corrected by subtracting the filter blank contents.

2.4. Data management

In order to analyze the influence of the air mass characteristics on the solubility of the particles, 4 days backward trajectories ending in Bobadela were calculated for all samples, with the Hy-splyt Model [25] from the National Oceanic and Atmospheric Administration (NOAA). In order to isolate air masses with higher marine aerosol content and air masses with higher mineral aerosol content, they were classified in three groups according to the backward trajectories: (1) Maritime air masses—if backward trajectories indicate an ocean origin, without continental contamination, during one of the previous 4 days; (2) South Continental air masses—if backward trajectories indicate an African or southern Europe origin, and (3) others—if backward trajectories do not have the previous characteristics (see Fig. 1).

Sources categories for $PM_{2.5}$ and $PM_{10-2.5}$ constituents were identified by means of Principal Component Factor Analysis (PCA) using STATISTICA software. This was performed by utilizing the orthogonal transformation method with Varimax rotation and retention of principal components whose eigenvalues were greater than unity. Factor loadings indicate the correlation of each pollutant species with each component and are related to the source emission composition. The contribution of each source group to some aerosol species was then quantitatively assessed by means of Multi Linear Regression Analysis (MLRA). MLRA was applied to the experimental data, using as dependent variables the species concentrations and as independent variables the principal component factor scores. As the factor scores obtained from the PCA are

normalized, with mean zero and standard deviation equal to unity, the true zero for each factor score was calculated by introducing an artificial sample with concentrations equal to zero for all variables. PCA was performed and the factor scores obtained for this artificial sample subtracted from the factor scores of each one of the other samples [26]. The details of the method and source apportionment results were given in previous works [17,27].

3. Results and discussion

Fig. 3 presents the average total APM and species concentration, for both fine and coarse fractions, and the techniques used for the determination of each species. The latter stresses the wide range of APM constituents that can be measured when k_0-INAA, PIXE and classical techniques are used.

The fine particulate mass concentration varied between 2.4 and 30 $\mu g\,m^{-3}$ and had a mean value of 14 $\mu g\,m^{-3}$. The coarse particulate mass concentration varied between 4 and 88 $\mu g\,m^{-3}$ and had a mean value of 18 $\mu g\,m^{-3}$. The most abundant species (concentrations generally higher than 1 $\mu g\,m^{-3}$) in APM were OC, SO_4^{2-}, NO_3^-, Cl^-, BC, Na^+, total Ca and NH_4^+.

The atmospheric aerosol size distribution is almost always bimodal in mass. Furthermore, the two modes have different origins. The coarse mode particles are often natural in origin, and are created in mechanical processes such as erosion of soil and sea spray. Anthropogenic activities, such as industrial or other combustion processes, are essentially responsible for the emission of fine mode particles [28]. Fig. 3 shows that for S, V, Ni, As, Se, Br, Sb, Pb, SO_4^{2-}, NO_3^-, NH_4^+, K^+, H^+, OC, and BC the fine fraction clearly had higher contents than the coarse fraction, indicating their provenance from anthropogenic activities. For the other elements, the coarse fraction was more important than the fine fraction. Al, Si, Ca, Sc, Ti, Fe, La, Ce and Sm reflect a soil fraction, whether naturally produced or re-suspended. Na and Cl were probably emanated from sea salt spray contributions.

These assumptions were confirmed by PCA analysis. Six main sources were identified to contribute to $PM_{2.5}$ levels. The first factor represented the crustal contribution defined by typical soil elements, such as Al, Si, Sc, Ti, Mn, Fe, Co,

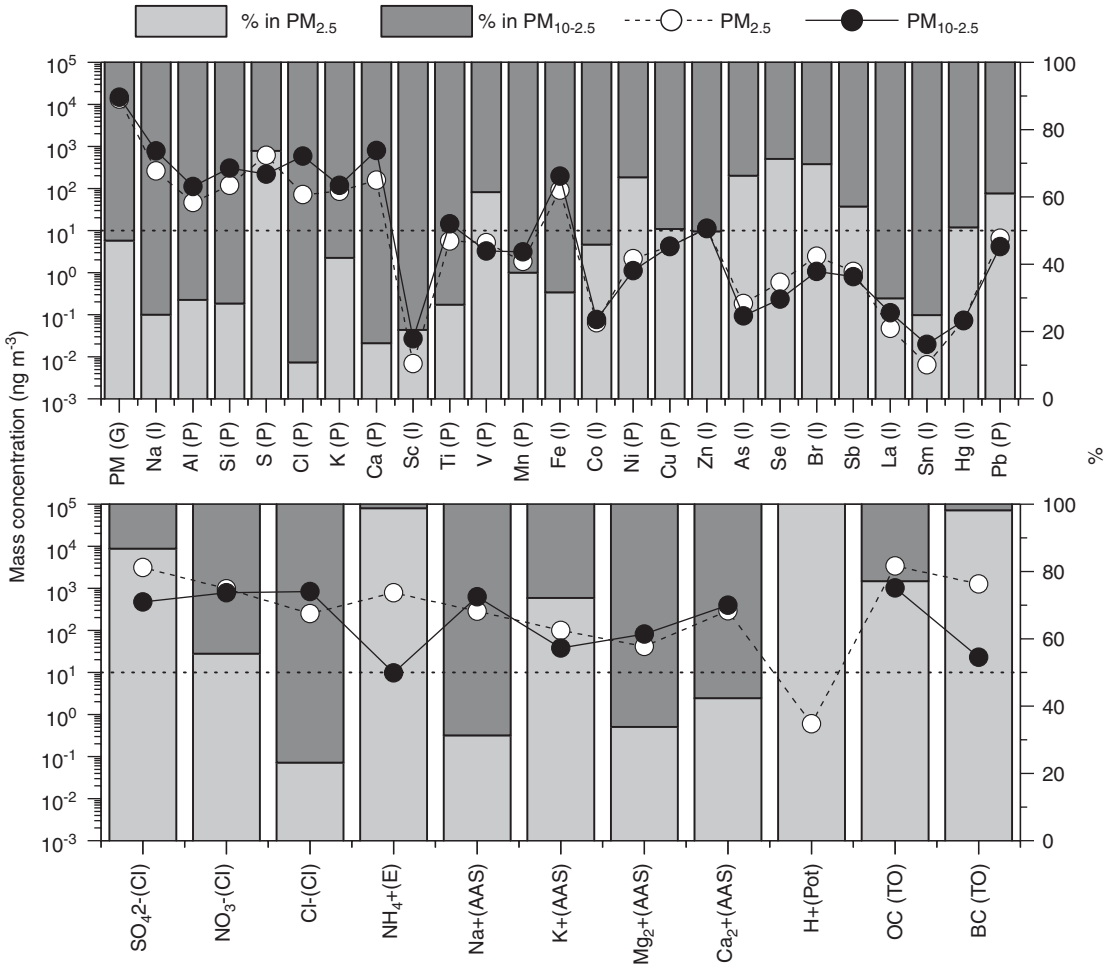

Fig. 3. $PM_{2.5}$ and $PM_{10-2.5}$ average concentrations at Bobadela (values in ng m^{-3}). Mass distribution of species in $PM_{2.5}$ and $PM_{10-2.5}$. G—gravimetry, I—k_0-INAA, P—PIXE, IC—ion chromatography, IS—indophenol-blue spectrophotometry, AAS—atomic absorption spectrophotometry, Pot—potentiometry, TO—thermo-optical method, OC—organic carbon, BC—black carbon.

La, Sm, Ca and K. The main components defining the second factor were V and Ni, which were derived from fuel oil combustion. The third factor represented the marine aerosol, as deduced from the high Na^+, Cl^- and Mg^{2+} loading factors. The main components defining the fourth factor were SO_4^{2-} and NH_4^+, which were derived from gas to particle conversion processes of products of SO_2 oxidation and NH_3. K presented some correlation (factor loading = 0.30) with the secondary aerosol factor. Cu, Zn, Sb and Pb were the main components defining the fifth factor, which usually originates from coal combustion, incineration and traffic (mainly brake wear and tires). Despite the reduced factor loadings, Ca (0.25) and K (0.20) also presented some correlation with this factor. Finally, the chemical profile of the sixth factor was mainly defined by NO_3^-, which derives from gas to particle conversion processes of products of the NO_x oxidation and derives mainly from motor vehicles. Potassium was also correlated with this factor (factor loading = 0.56).

In the coarse fraction, five sources were identified to contribute to $PM_{10-2.5}$. The first source represented the crustal contribution, defined by Al, Si, Sc, Ti, Mn, Fe, Co, La, Sm, insoluble K and Ca (soluble and insoluble). The second factor represented the marine aerosol, as indicated by the high Na^+, Cl^- and Mg^{2+} factor loading. Soluble potassium and sulfur had also a high factor loading for this factor. The main components defining the third component were V and Ni, which provided from fuel oil combustion. The chemical profile of the fourth factor was defined by SO_4^{2}, NH_4^+ and NO_3^-, which derive from gas-to-particle conversion processes. Soluble calcium was also associated with this factor. Finally, the main components defining the fifth factor were Cu, Zn, Sb, Pb and Ca (soluble and insoluble). This factor is probably associated to coal combustion, traffic and incineration.

In Fig. 4, chlorine, sodium, sulphur, potassium and calcium elemental concentrations are compared with the concentration of Cl^-, Na^+, SO_4^{2-}, K^+ and Ca^+ water soluble ions. Table 1 shows the average ratio between elemental and water soluble concentrations for $PM_{2.5}$, $PM_{10-2.5}$ and PM_{10}, discriminated by air mass type.

3.1. Chlorine

Cl was not measured by k_0-INAA because only a long irradiation was performed to determine medium and long lived radionuclides. Therefore, Cl results were provided from PIXE analysis.

Compared with total Cl measured by PIXE, higher concentrations were registered for water soluble Cl, measured by IC. This means that part of the element Cl was depleted.

Losses of halogens (especially Cl) from aerosols during sampling, sample storage and analysis have been reported and discussed by various authors [29–31]. The extent of the loss depends on several factors, including the sampling device used, the size fraction, the composition of the aerosol, the chemical form of the particulate halogen, the presence of acidic species—HNO_3, H_2SO_4—in the air sampled, the duration of the sample storage and the analytical technique used [32].

PCA, applied to fine and coarse fractions, showed that Cl was associated with a marine aerosol component defined by sodium, chlorine and magnesium. However, a Cl depletion was verified when Cl/Na aerosols ratio and Cl/Na bulk sea water ratio (1.8) were compared. Similar results were obtained by several authors [33–35].

The relationship between Cl^- and Na^+ and Cl and Na total concentrations in fine and coarse aerosol is shown in Fig. 5. The least-squares lines regression fitting parameters for the data are presented in Table 2. It is clear that Cl is strongly associated to Na in the coarse fraction. In the fine aerosol fraction, nearly all the points are below the bulk sea water line, indicating strong Cl depletion. The deficit is a result of the NaCl reaction with acidic species leading to a displacement of Cl^- as HCl. The latter is strongly supported by the negative Cl factor loading associated with the secondary aerosol principal component. The referred reaction is more efficient for smaller particles, most likely due to a higher surface-to-volume ratio and to higher coagulation rates [36]. This effect should be observed to the same extent for the relationship between ions and between elements. However, a higher depletion was observed for the comparison between elements. The low Cl/Cl^- ratio, observed especially in fine fraction, could be attributed to the volatilization of Cl during Nuclepore filters PIXE bombardment made in vacuum, already observed in other studies [30–32].

Cl loss in PIXE analysis is quite important in polluted air for the fine size fraction. Coarse Cl was volatized to a much lesser extent. The higher mean Cl/Cl^- ratios, for fine Cl, in samples associated to maritime air masses (0.64) compared with those found in samples associated to continental air masses (0.45) are mostly likely due to the higher level of pollution in the second ones. For the same reason, Cl volatilization depends clearly on the region where the samples were collected. This work refers to a sub-urban area and Cl/Cl^- ratios obtained were 0.49 and 0.69 for $PM_{2.5}$ and $PM_{10-2.5}$, respectively. In an urban residential site situated in Gent, Maenhaut and Cafmeyer [32] obtained an average Cl/Cl^- ratio of 0.32 for fine fraction, and 0.92 for coarse fraction. In Santiago do Chile, Toro and Cortés [31] obtained a Cl/Cl^- ratio of 0.23 for PM_{10}. In the South of Africa, in an unpolluted area, Salma et al. [30] found an average Cl/Cl^- ratio of 0.76 for fine fraction and 0.90 for coarse fraction.

3.2. Sodium

PCA applied to fine and coarse fractions indicated that the main source of Na is the sea. Fig. 4 shows higher Na concentrations for maritime air masses.

The relationship between total Na, measured by INAA, and water soluble Na^+, determined by AAS, shows that

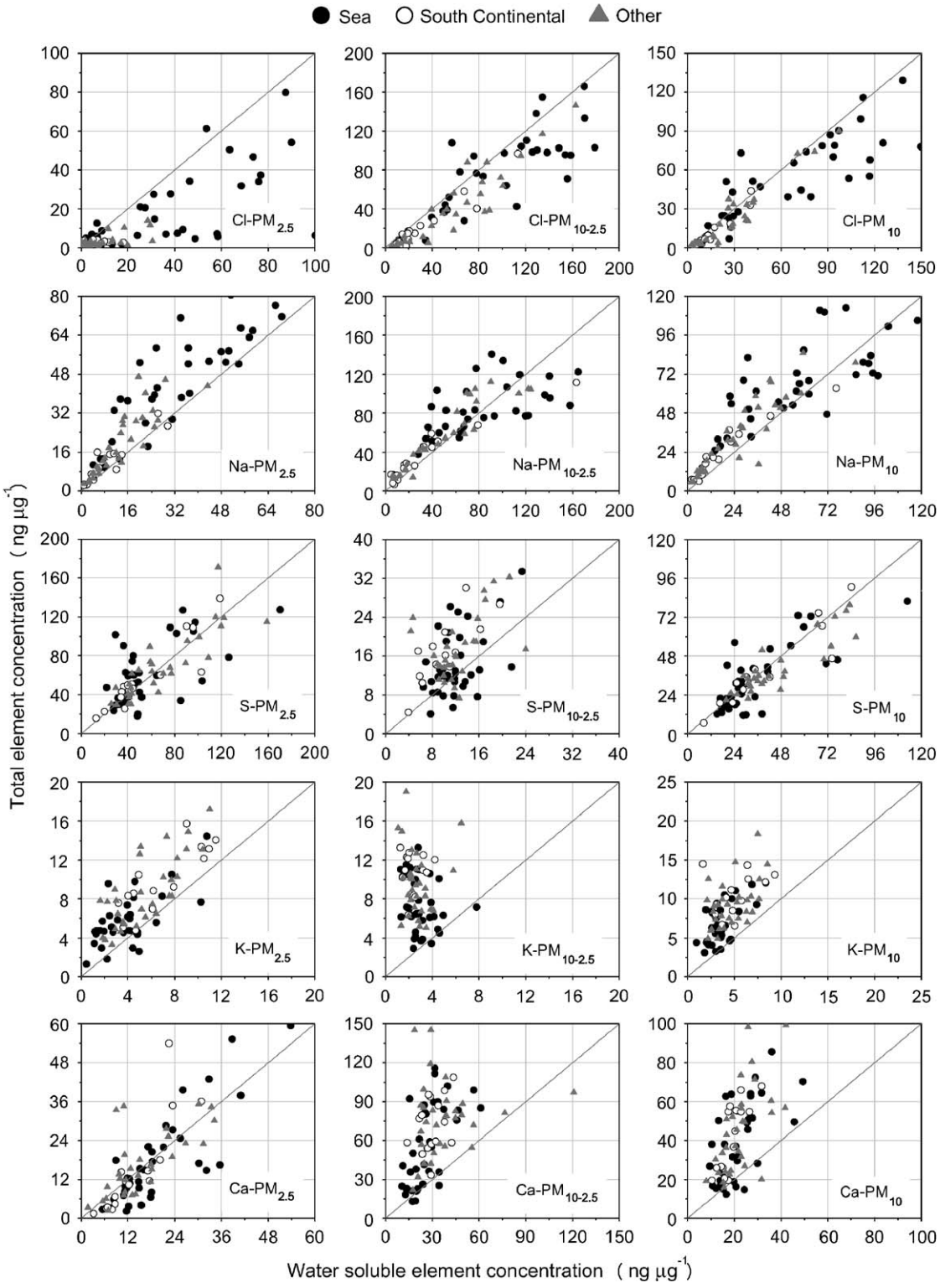

Fig. 4. Relationship between total and water soluble element concentration for chlorine, sodium, sulfur, potassium and calcium and for $PM_{2.5}$, $PM_{10-2.5}$ and PM_{10}, discriminated by air mass type. Data presented in ng μg^{-1}.

both fine and coarse fractions have a good solubility. However, samples associated to maritime air masses, mainly in the coarse fraction, present higher sodium solubility, the average Na/Na^{+} ratio being 1.0. These results show that the chemical form associated to sea salt spray is very soluble, whereas other forms—mainly associated to fine fraction and probably with anthropogenic origin—present a weaker solubility.

3.3. Sulfur

The total sulfur, measured by PIXE, was compared with water soluble sulfur, determined via SO_4^{2-} mass, which was analyzed by IC. In the fine fraction, PCA identified a component defined by SO_4^{2-} and NH_4^+, which were originating from gas-to-particle conversion processes of products of the SO_2 oxidation and NH_3. The relationship between total sulfur and sulfur determined via sulfate is very good, showing that the majority of the sulfur is in the sulfate form.

In the coarse fraction, the agreement between total and soluble sulfur is not so good, mainly for non-maritime air masses. In $PM_{10-2.5}$, PCA indicated that SO_4^{2-} is associated with both (1) a component defined by SO_4^{2-}, NH_4^+ and NO_3^-, which derive from gas-to-particle conversion processes and (2) a marine aerosol component defined by sodium, chloride, magnesium, SO_4^{2-} and soluble potassium. A better agreement between total sulfur and sulfate was obtained for samples associated with sea trajectories. This indicates that the sulfur chemical form resulting from sea spray is very soluble.

Table 1
Ratio between total and water soluble element concentrations for chlorine, sodium, sulfur, potassium and calcium

		Total	Sea	South Cont.	Other
Cl	$PM_{2.5}$	0.49	0.64	0.45	0.37
	$PM_{10-2.5}$	0.69	0.77	0.71	0.60
	PM_{10}	0.72	0.84	0.69	0.68
Na	$PM_{2.5}$	1.4	1.3	1.5	1.5
	$PM_{10-2.5}$	1.2	1.0	1.3	1.3
	PM_{10}	1.4	1.2	1.6	1.5
S	$PM_{2.5}$	1.1	1.1	1.2	0.97
	$PM_{10-2.5}$	1.4	1.1	1.7	1.4
	PM_{10}	0.96	1.0	1.0	0.94
K	$PM_{2.5}$	1.5	1.5	1.4	1.5
	$PM_{10-2.5}$	3.4	2.1	3.9	3.7
	PM_{10}	1.8	1.7	1.9	1.8
Ca	$PM_{2.5}$	0.91	0.87	0.84	0.98
	$PM_{10-2.5}$	2.0	1.9	2.5	1.8
	PM_{10}	1.9	1.7	2.1	2.1

Average calculated for all the samples (Total), samples associated to maritime air masses (Sea), south continental air masses (South Cont.) and the remaining air masses (Other).

3.4. Potassium

In the fine fraction, the average K/K^+ ratio was 1.5 and the differences between air masses trajectories were not significant. PCA applied to the fine fraction aerosol components showed that potassium is associated to anthropogenic sources—road traffic and combustion processes.

In the coarse fraction, results presented in Table 1 show that potassium had a weaker solubility, especially for the non-maritime air masses. The samples associated to South Continental air masses—characterized by high contents of mineral aerosols transported from the North of Africa and South of Europe—had the highest average K/K^+ ratio (3.9).

In the coarse fraction, soil and sea spray were the most important sources for potassium. PCA showed that soluble potassium—associated with Cl^-, Na^+ and Mg^{2+}—is correlated with sea spray; while insoluble potassium—associated mainly with soil elements such as Al, Si, Sc, Ti, Mn, Fe,

Table 2
Least-squares linear regression fitting parameters for the relationship between Cl and Na and for the relationship between Cl^- and Na^+, for fine and coarse fractions

		Slope	Interception	r
Fine	Cl/Na	0.76	−120	0.79
	Cl^-/Na^+	1.1	−9.1	0.69
Coarse	Cl/Na	1.2	−170	0.91
	Cl^-/Na^+	1.5	−86	0.91

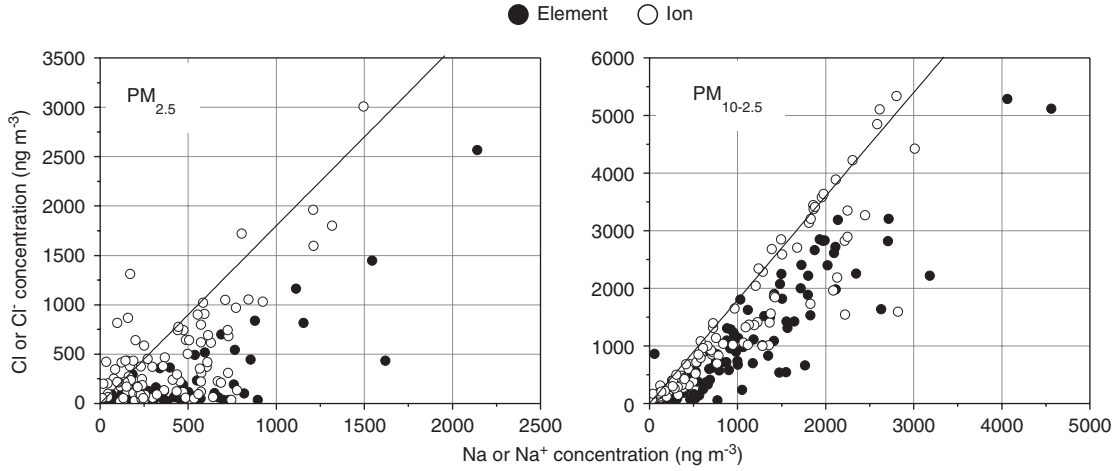

Fig. 5. Relationship between chlorine and sodium concentration for total and water soluble element concentration and for $PM_{2.5}$ and $PM_{10-2.5}$.

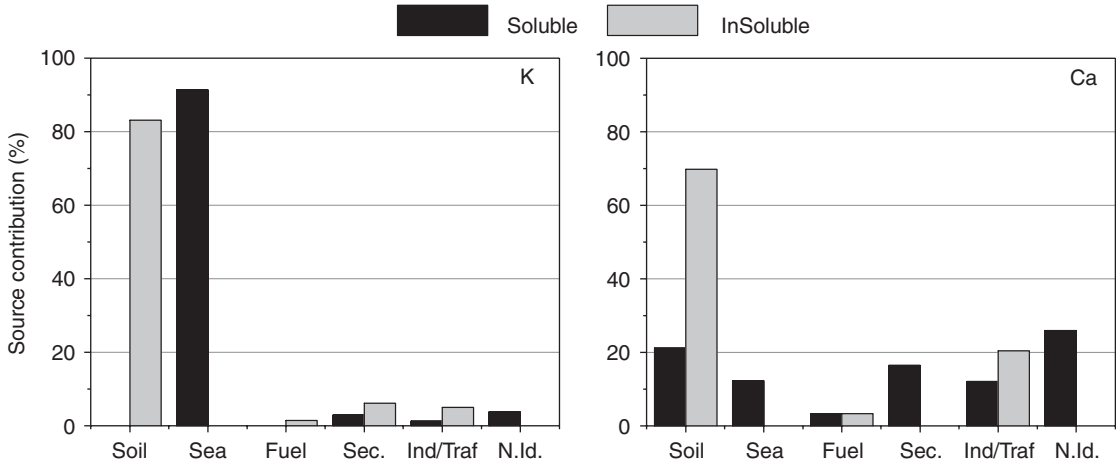

Fig. 6. Quantitative contribution of each source group, identified by PCA, for coarse soluble and insoluble potassium and calcium concentration (Sec—Secondary aerosols, Ind/Traf—Industry and Traffic, N.Id.—Non identified).

Co, La and Sm—is correlated with mineral aerosol. To assess quantitatively the contribution of each source group to the soluble and insoluble potassium, a MLRA was applied to the experimental data, using as dependent variables the soluble and insoluble potassium concentrations and as independent variables the principal component factor scores. Fig. 6 shows that, on the average, the largest contribution to the soluble potassium concentration in coarse fraction was the sea (91%), which did not contribute to the concentration of insoluble potassium. The soil was the most important source for the coarse insoluble potassium, contributing, on the average, for 83% of the mass. According to Watson and Chow [37] the abundance of total potassium is approximately 10 times the abundance of soluble potassium in all geological profiles studied by them.

3.5. Calcium

PCA applied to the fine fraction aerosol components showed a correlation between calcium and the soil and combustion processes sources. For this granulometry, a good agreement between total calcium (measured by PIXE) and soluble Ca (measured by AAS) was found, showing a very good solubility. The average Ca/Ca^{2+} ratio (0.91) indicates that PIXE was underestimating the Ca concentration, which is compatible with the results obtained in the analysis of the standard filter NIST-SRM 2783 (measured/certified ratio $= 0.76 \pm 0.19$, see Fig. 2)[17,20].

In the coarse fraction, the solubility was weaker mainly for samples associated with South Continental trajectories which are rich in mineral particulates contents. In mineral aerosol, calcium could be associated with aluminum and silicium resulting in insoluble species. However, calcium carbonate, which has a solubility of $1.4 \times 10^{-5}\,g\,mL^{-1}$ is also a very frequent compound in mineral aerosol. Fig. 6 shows that the soil presents the highest contribution for the insoluble calcium (70%). Moreover, the factor associated with industry and traffic, identified by Cu, Zn, Sb and Pb, had also a significant contribution for insoluble calcium (20%). Soluble calcium is not only associated to the soil (21%) but also to the secondary aerosols (16%). In warmer seasons, minor amounts of ammonium-nitrate are expected, and the occurrence of NO_3^- is mainly attributed to the reaction of gaseous HNO_3^- with mineral species such as calcium carbonate to form $Ca(NO_3)_2$.

4. Conclusion

When aerosol analysis is required, k_0-INAA and PIXE are very good techniques to solve the analytical problem. The advantage of these methods, comparing with IC and AAS, is the fact that they use solid samples. Therefore, no special handling is necessary prior to analysis avoiding the introduction of contaminations and errors associated with the digestion. Aerosol samples are associated with small masses and quite low concentrations of elements. Thus, the determination of a large number of elements is not a trivial task. k_0-INAA and PIXE are multi-element techniques, implying that only one sample and measurement is necessary to quantify many elements. Moreover, they have proven to be in a good position to tackle aerosol measurements because very low detection limits can be achieved. Classical non-nuclear techniques are an essential tool to determine the concentration of some important environmental aerosol species like SO_4^{2-}, NH_4^+ and NO_3^-.

The multi-technique analytical approach, using nuclear and classical techniques, not only provided results for a large number of APM species (essential for source apportionment studies) but, for several elements, independent methods also gave information about their solubility. The information about total and soluble fraction concentrations of an element could be used (1) to find inaccuracies due to methods bias (for instance Cl depletion in PIXE analysis) and (2) to differentiate sources associated to the soluble or insoluble fractions.

Chlorine volatilization during PIXE Nuclepore filters bombardment made in vacuum may be important for the fine fraction in polluted air.

Sodium, provided mainly from sea salt spray, presented a very good solubility.

Both fine and coarse sulfur were mainly associated with secondary aerosol. However, in the coarse fraction, sea spray also contributed to its concentrations. In PM_{10} the majority of the sulfur was in SO_4^{2-} chemical form.

In the coarse fraction, potassium had mainly a natural origin—soil and sea spray. The study of the potassium solubility was essential to isolate the contribution of each of these sources. The sea contribution was identified by soluble potassium, whereas mineral aerosol is principally associated with insoluble potassium.

The average Ca/Ca^{2+} ratio indicates that PIXE was underestimating the Ca concentration. In the coarse fraction, calcium presented a lower solubility. This was attributed to the higher mineral contribution registered in this granulometry.

Acknowledgements

The authors thank Fundação para a Ciência e Tecnologia the fellowships PRAXIS XXI/BD/19801/99 and SFRH/BPD/14479/2003.

References

[1] J. Schwartz, Environ. Res. 62 (1993) 7.
[2] D.W. Dockery, C.A. Pope, X. Xu, J.D. Spengler, J.H. Ware, M.E. Fay, B.G. Ferris, F.E. Speizer, New Engl. J. Med. 329 (1993) 1753.
[3] C.A. Pope, R.T. Burnett, M.J. Thun, E.E. Calle, D. Krewski, K. Ito, G.D. Thurston, J. Am. Med. Assoc. 287 (2002) 1132.
[4] T. Reichhardt, Environ. Sci. Technol. 29 (1995) 360.
[5] D.J. Swaine, Fuel Process Technol 65 (2000) 21.
[6] T.A. Pakkanen, K. Loukkola, C.H. Korhonen, M. Aurela, T. Mäkelä, R.E. Hillamo, P. Aarnio, T. Koskentalo, A. Kousa, W. Maenhaut, Atmos. Environ. 35 (2001) 5381.
[7] Y.C. Chan, R.W. Simpson, G.H. Mctainsh, P.D. Vowles, D.D. Cohen, G.M. Bailey, Atmos. Environ. 33 (1999) 3251.
[8] W. Chueinta, P.W. Hopke, P. Paatero, Atmos. Environ. 34 (2000) 3319.
[9] C.A. Pio, L.M. Castro, M.A. Cerqueira, I.M. Santos, F. Belchior, M.L. Salgueiro, Atmos. Environ. 30 (1996) 3309.
[10] X. Querol, A. Alastuey, S. Rodriguez, F. Plana, C.R. Ruiz, N. Cots, G. Massagué, O. Pluig, Atmos. Environ. 35 (2001) 6407.
[11] A.V. Polissar, P.K. Hopke, R.L. Poirot, Environ. Sci. Technol. 35 (2001) 4604.
[12] W. Maenhaut, The "Gent" stacked filter unit (SFU) sampler for the collection of atmospheric aerosols in two size fractions: description and instructions for installation and use, IAEA CRP E4.10.08, Belgium, 1992.
[13] R.L. Tanner, W.H. Marlow, L. Newman, Environ. Sci. Technol. 13 (1979) 75.
[14] H.J.M. Bowen, D. Gibbons, Radioactivation Analysis, Clarendon, Oxford, 1963.
[15] F. De Corte, The K_0-standardization method—a move to the optimization of neutron activation analysis, Agregé Thesis, Gent University, Gent, 1987.
[16] S.A.E. Johansson, J.L. Campbell, PIXE—A novel technique for elemental analysis, Wiley, New York, 1988.
[17] S.M. Almeida, Composition and sources of atmospheric aerosol in an urban/industrial region, Ph.D. Thesis, Aveiro University, Portugal 2004 [in Portuguese].
[18] S.M. Almeida, M.A. Reis, M.C. Freitas, C.A. Pio, Nucl. Instr. and Meth. B 207 (2003) 434.
[19] S.M. Almeida, M.C. Freitas, M.A. Reis, C.A. Pio, J. Radioanal. Nucl. Chem 257 (2003) 609.
[20] M.C. Freitas, M.M. Farinha, M.G. Ventura, S.M. Almeida, M.A. Reis, A.M.G. Pacheco, J. Radioanal. Nucl. Chem. 263 (2005) 711.
[21] J.C. Chow, J.G. Watson, Ion chromatography in elemental analysis of airborne particles, in: S. Landsberger, M. Creatchman (Eds.), Elemental Analysis of Airborne Particles. Advances in Environmental, Industrial and Process Control Technologies, vol. 1, Gordon and Breach, USA, 1999, p. 97.
[22] M.W. Weatherburn, Anal. Chem. 39 (1967) 971.
[23] P.M. Grohse, Trace element analysis of airborne particles by atomic absorption spectroscopy, inductively coupled plasma-atomic emission spectroscopy, and inductively coupled plasma-mass spectroscopy, in: S. Landsberger, M. Creatchman (Eds.), Elemental Analysis of Airborne Particles. Advances in Environmental, Industrial and Process Control Technologies, vol. 1, Gordon and Breach, 1999, p. 1.
[24] C.A. Pio, L.M. Castro, M.O. Ramos, in: Proceedings of the Sixth European Symposium on Physical–Chemical Behaviour of Atmospheric Pollutants, 1993, p. 706.
[25] R.R. Draxler, Hybrid Single-Particle Lagrangian Integrated Trajectories, Version 3.2, NOAA-ARL, 1994.
[26] G.D. Thurston, J.D. Spengler, J. Clim. Appl. Meteorol. 24 (1985) 1245.
[27] S.M. Almeida, C.A. Pio, M.C. Freitas, M.A. Reis, M.A. Trancoso, Atmos. Environ. 39 (1995) 3127.
[28] F. Raes, R. Van Dingenen, E. Vignati, J. Wilson, J.-P. Putaud, J.H. Seinfeld, P. Adams, Atmos. Environ. 34 (2000) 4215.
[29] W. Maenhaut, H. Raemdonck, M.O. Andreae, Nucl. Instr. and Meth. B 22 (1987) 248.
[30] I. Salma, W. Maenhaut, H.J. Annegarn, M.O. Andreae, F.X. Meixner, M. Garstang, J Radioanal. Nucl. Chem. 216 (1997) 143.
[31] P. Toro, E. Cortés, J. Radioanal. Nucl. Chem. 221 (1997) 127.
[32] W. Maenhaut, J. Cafmeyer, X-ray Spectrom. 27 (1998) 236.
[33] C.A. Pio, M.A. Cerqueira, L.M. Castro, M.L. Salgueiro, Atmos. Environ. 30 (1996) 3115.
[34] V.-M. Kerminen, K. Teinilä, R. Hillamo, Atmos. Environ. 34 (2000) 2817.
[35] B. Roth, K. Okada, Atmos. Environ. 32 (1998) 1555.
[36] R.M. Harrison, C.A. Pio, Atmos. Environ. 17 (1983) 1733.
[37] J.G. Watson, J.C. Chow, Sci. Total Environ. 276 (2001) 33.